

AD-A224 278

DTIC FILE COPY

1

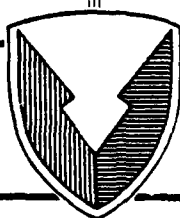
TECHNICAL REPORT CR-RD-RE-90-1

**FARADAY ROTATION MAPPING OF MERCURY
CADMIUM TELLURIDE**

DTIC
S ELECTE **D**
JUL 25 1990
CgD

G. A. Tanton
C. R. Christensen
J. A. Grisham
Research, Development, and Engineering Center
and
J. A. Stensby
Department of Electrical and Computer Engineering
University of Alabama in Huntsville
Huntsville, AL

MARCH 1990



U.S. ARMY MISSILE COMMAND

Redstone Arsenal, Alabama 35898-5000

Approved for public release; distribution is unlimited.

DISPOSITION INSTRUCTIONS

DESTROY THIS REPORT WHEN IT IS NO LONGER NEEDED. DO NOT RETURN IT TO THE ORIGINATOR.

DISCLAIMER

THE FINDINGS IN THIS REPORT ARE NOT TO BE CONSTRUED AS AN OFFICIAL DEPARTMENT OF THE ARMY POSITION UNLESS SO DESIGNATED BY OTHER AUTHORIZED DOCUMENTS.

TRADE NAMES

USE OF TRADE NAMES OR MANUFACTURER'S IN THIS REPORT DOES NOT CONSTITUTE AN OFFICIAL ENDORSEMENT OR APPROVAL OF THE USE OF SUCH COMMERCIAL HARDWARE OR SOFTWARE.

UNCLASSIFIED

SECURITY CLASSIFICATION OF THIS PAGE

REPORT DOCUMENTATION PAGE

Form Approved
OMB No 0704-0188
Exp. Date: Jun 30, 1986

1a. REPORT SECURITY CLASSIFICATION Unclassified			1b. RESTRICTIVE MARKINGS			
2a. SECURITY CLASSIFICATION AUTHORITY			3. DISTRIBUTION / AVAILABILITY OF REPORT Approved for public release; distribution is unlimited			
2b. DECLASSIFICATION / DOWNGRADING SCHEDULE						
4. PERFORMING ORGANIZATION REPORT NUMBER(S) CR-RD-RE-90-1			5. MONITORING ORGANIZATION REPORT NUMBER(S)			
6a. NAME OF PERFORMING ORGANIZATION Research Directorate Res, Dev, and Eng Center		6b. OFFICE SYMBOL (If applicable) AMSMI-RD-RE-OP	7a. NAME OF MONITORING ORGANIZATION			
6c. ADDRESS (City, State, and ZIP Code) Commander U.S. Army Missile Command Redstone Arsenal, AL. 35898-5252			7b. ADDRESS (City, State, and ZIP Code)			
8a. NAME OF FUNDING / SPONSORING ORGANIZATION		8b. OFFICE SYMBOL (If applicable)	9. PROCUREMENT INSTRUMENT IDENTIFICATION NUMBER			
8c. ADDRESS (City, State, and ZIP Code)			10. SOURCE OF FUNDING NUMBERS			
			PROGRAM ELEMENT NO.	PROJECT NO.	TASK NO.	WORK UNIT ACCESSION NO.
11. TITLE (Include Security Classification) Faraday Rotation Mapping Of Mercury Cadmium Telluride						
12. PERSONAL AUTHOR(S) Tanton, G.A., Christensen, C.R., Grisham, J.A., Stensby, J.						
13a. TYPE OF REPORT Technical Report		13b. TIME COVERED FROM 89 Aug. TO 89 Dec.	14. DATE OF REPORT (Year, Month, Day) 90 March		15. PAGE COUNT 25	
16. SUPPLEMENTARY NOTATION						
17. COSATI CODES			18. SUBJECT TERMS (Continue on reverse if necessary and identify by block number)			
FIELD	GROUP	SUB-GROUP	Faraday Rotation, Mercury Cadmium Telluride			
19. ABSTRACT (Continue on reverse if necessary and identify by block number) This report summarizes the application of Faraday Rotation (FR) to determine the uniformity of free-carrier concentrations in samples of Mercury Cadmium Telluride as a function of position. This effort is the first application of FR measurement techniques on tertiary compounds. The results presented, demonstrate first order agreement of the technique with Hall measurements performed at cryogenic temperatures. Further studies and development of calibration standards are recommended.						
20. DISTRIBUTION / AVAILABILITY OF ABSTRACT <input checked="" type="checkbox"/> UNCLASSIFIED/UNLIMITED <input type="checkbox"/> SAME AS RPT. <input type="checkbox"/> DTIC USERS			21. ABSTRACT SECURITY CLASSIFICATION Unclassified			
22a. NAME OF RESPONSIBLE INDIVIDUAL Mr. G.A. Tanton			22b. TELEPHONE (Include Area Code) (205) 876-3820		22c. OFFICE SYMBOL AMSMI-RD-RE-OP	

PREFACE

This report summarizes the efforts performed in the Research Directorate, MICOM during the period from August 1989 to the end of December 1989, to demonstrate the feasibility of using the Faraday rotation technique to map free carrier concentrations in both bulk grown and epitaxially grown mercury cadmium telluride substrates.

The support for this effort was provided by the Systems Engineering and Production Directorate Manufacturing Technology Division's Manufacturing Science program, and by the Research Directorate.



Accession For	
NTIS CRA&I	<input checked="checked" type="checkbox"/>
DTIC TAB	<input type="checkbox"/>
Unannounced	<input type="checkbox"/>
Justification	
By	
Distribution /	
Availability Codes	
Dist	Avail and/or Special
A-1	

ACKNOWLEDGMENTS

The cooperation extended by the Center for Night Vision Electro-Optics (CNVEO), CE-COM, by providing the MCT samples and Hall data used in Table 1, taken by Michael Grenn (CNVEO), is acknowledged. The work reported here was made possible through the support of the Systems Engineering and Production Directorate Manufacturing Technology Division's Manufacturing Science program and by the Research Directorate, MICOM. Technical assistance of Rachel Wright is gratefully acknowledged.

TABLE OF CONTENTS

	Page
LIST OF ILLUSTRATIONS	vi
I. INTRODUCTION	1
II. EXPERIMENTAL SETUP	2
III. BACKGROUND THEORY	5
IV. RESULTS	6
V. COMPARISONS	13
VI. CONCLUSIONS AND RECOMMENDATIONS	14
APPENDIX – OPERATIONAL DETAILS OF THE FARADAY ROTATION POLARIZER/ANALYZER COMBINATION	A-1

LIST OF ILLUSTRATIONS

<u>Figure</u>	<u>Title</u>	<u>Page</u>
1	Faraday Rotation Mapper (Bench Setup)	2
2	Faraday Rotation Mapper	3
3	Faraday Rotation Optical Train	3
4	Split Magnet for FR Measurements	4
5	Relative Sizes of MCT Used in FR Demonstration	6
6	Faraday Rotation Signal vs Magnetic Field Strength	7
7	Faraday Rotation in MCT4 @ 300 K Repeatability Test	7
8	System Initialization Setup Without Sample	7
9	Dectector Output Versus Analyzer Angle No Sample	8
10	Faraday Rotation Signal vs Analyzer Angle for MCT4 AT 300k ..	8
11	Faraday Rotation Signal vs Tangent of Analyzer Angle	9
12	FR Signal vs Tan ($\theta-3$)	10
13	Low Resolution Map of MCT4 (20 Data Points)	11
14	High Resolution Map of MCT4 (63 Data Points)	12

I. INTRODUCTION

The technique of Faradary Rotation (FR), which is established as a scientific research tool for binary semiconductors [1, 2] is extended in this work to the tertiary compound mercury cadmium telluride (MCT).

Our objective is to develop innovative noncontact methods that can be applied in medium and long wavelength infrared detector manufacturing to increase yield, reduce production costs, and to improve traceability throughout the manufacturing process.

Conventional methods used to characterize semiconductor material do not quickly or efficiently identify areas of a wafer that will produce useful detectors for focal plane arrays. This results in lower production yields and higher unit cost. In the technique described herein the material of interest is positioned in an amplitude modulated magnetic field and scanned with a linearly polarized laser beam. As the laser beam passes through the material it undergoes Faraday rotation proportional to the free carrier concentration in that particular part of the wafer. Since the detector device characteristics, such as effective resistance and capacitance, are functions of the free carrier concentration, parts of a wafer that will not yield good detectors can be identified in the early stages of manufacturing using this technique. The yield would be significantly increased and the unit cost decreased by identifying and culling wafers or parts of wafers; that do not meet specifications at the beginning of the fabrication process. It is expected that this FR technique can be utilized as a universal evaluation tool that will make manufacturing traceability possible by correlating device performance for any part of a wafer with fundamental parameters. This technique is applicable to all major detector materials of Army interest, e.g., mercury cadmium telluride (HgCdTe), indium antimonide (InSb), platinum silicate (PtSi), and gallium arsenide (GaAs).

Major advantages of this technique are: a) no contacts need be alloyed with the wafer, hence no wafer material contamination; b) surface preparation is not required; c) it is a rapid computer controlled technique and does not require a skilled operator; and d) automated wafer mapping is possible. An objective of the effort reported here is to demonstrate the applicability of FR for the measurement of electronic homogeneity of MCT wafers. The first steps in accomplishing this goal appear to be successful. The method, apparatus, and measurement results to date are reported here. Although these results are limited at present to only a few samples measured at ambient temperature, extensive measurements on the bulk material demonstrate the method for MCT. Much of the initial effort has focused on developing the instrumentation. Future improvements now in the design phase include the addition of a cryogenic capability and a longer wavelength source to map wafers at 77 K.

II. EXPERIMENTAL SETUP

Figure 1 is an overall view of the bench set-up that is shown schematically in Figure 2.

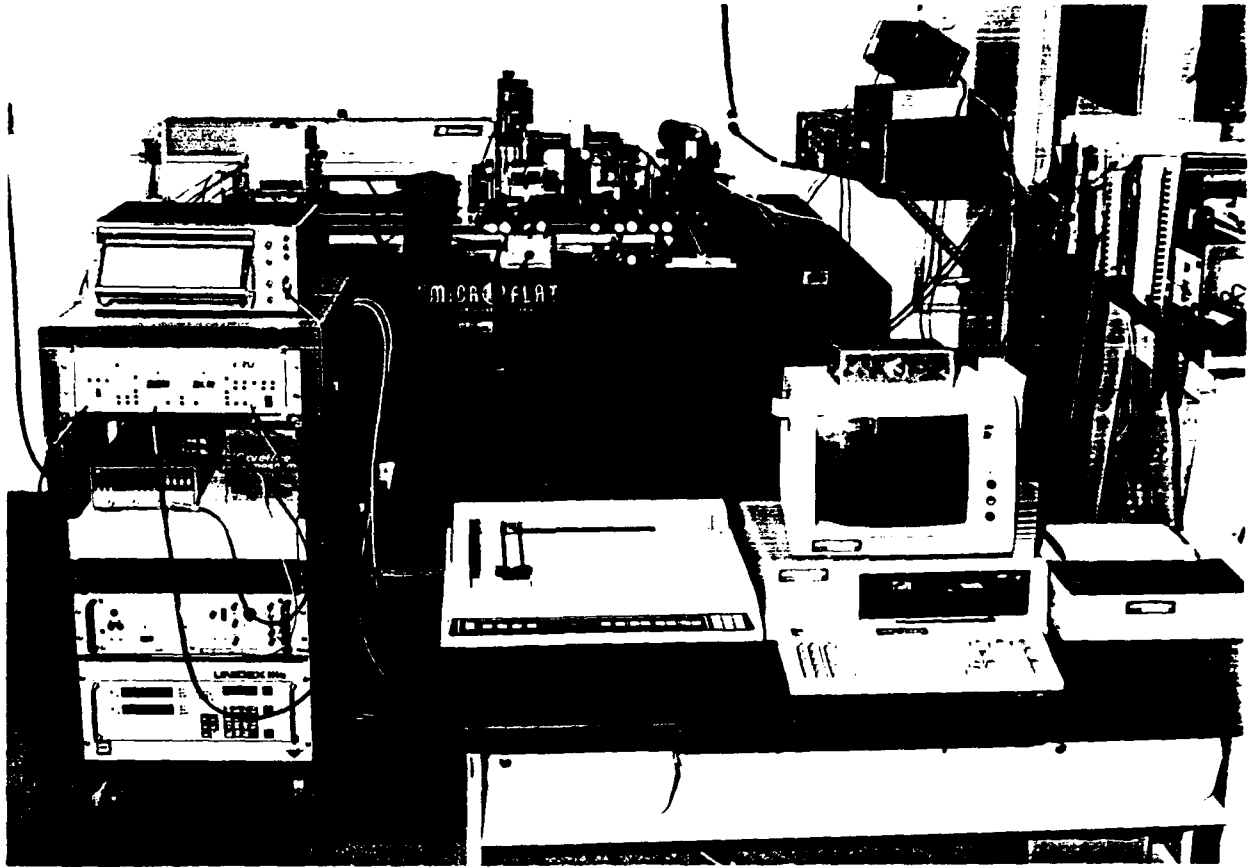
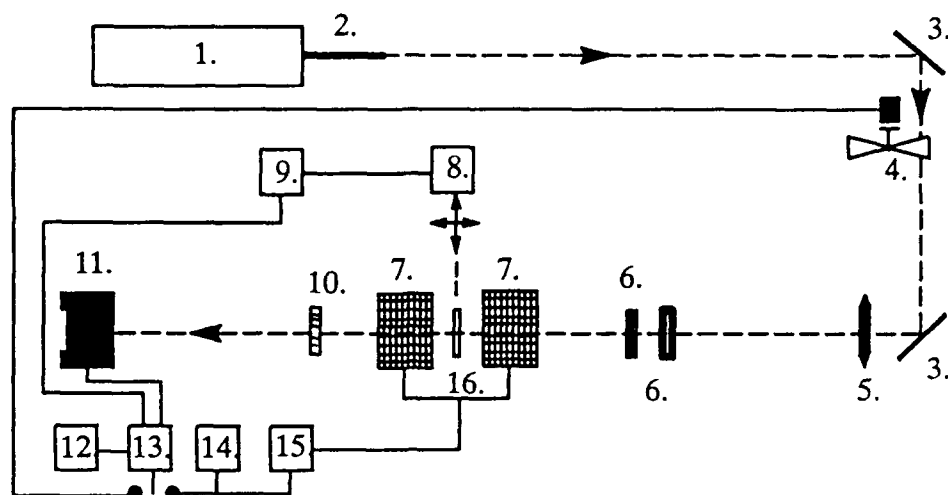


Figure 1. Faraday Rotation Mapper (Bench Setup).

The wafer was probed with a 2 mW CO₂ laser beam at a wavelength of 10.6 micrometers. The sample was positioned in a magnetic field by X/Y translation stages with a positioning precision of 0.005 mm. The free carrier concentration in a particular part of the wafer was determined by the Faraday rotation as the laser beam passed through the material. The reference plane of polarization was established by two wire grid ZnSe polarizers shown in Figure 3 and an analyzer, rotated at a bias angle θ , was placed after the wafer.



1. LASER, 2 WATTS CW @ 10.6 MICRONS	2 ATTENUATOR
3. MIRROR	4. CHOPPER
5. FOCUSING LENS	6. POLARIZER, ZnSe WIRE GRID
7. SPLIT ELECTRO-MAGNET, 2.4 kG	8. X/Y TRANSLATION STAGES
9. IBM PC	10. ANALYZER, ZnSe
11. DETECTOR, HgCdTe @ 77 K	12. RECORDER, STRIP CHART
13. LOCK-IN, AMPLIFIER	14. SINE WAVE GENERATOR
15. MAGNET DRIVER POWER AMPLIFIER	16. SAMPLE

Figure 2. Faraday Rotation Mapper.

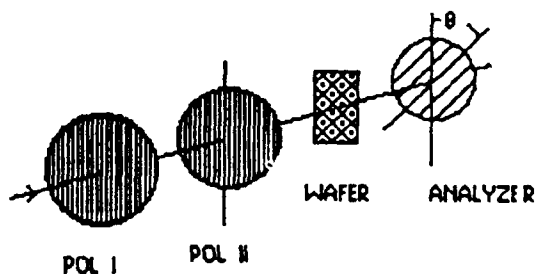


Figure 3. Faraday Rotation Optical Train.

A 25 mm focal length ZnSe lens in front of polarizer I focused the beam to 0.3 mm diameter at the wafer, resulting in a flux density of $10 - 50 \text{ W/cm}^2$. The split magnet shown in Figure 4 produced a 10 Hz amplitude modulated magnetic field of $\pm 2.4 \text{ kG}$. The magnetic field was directed parallel to the propagation axis of the probe beam.

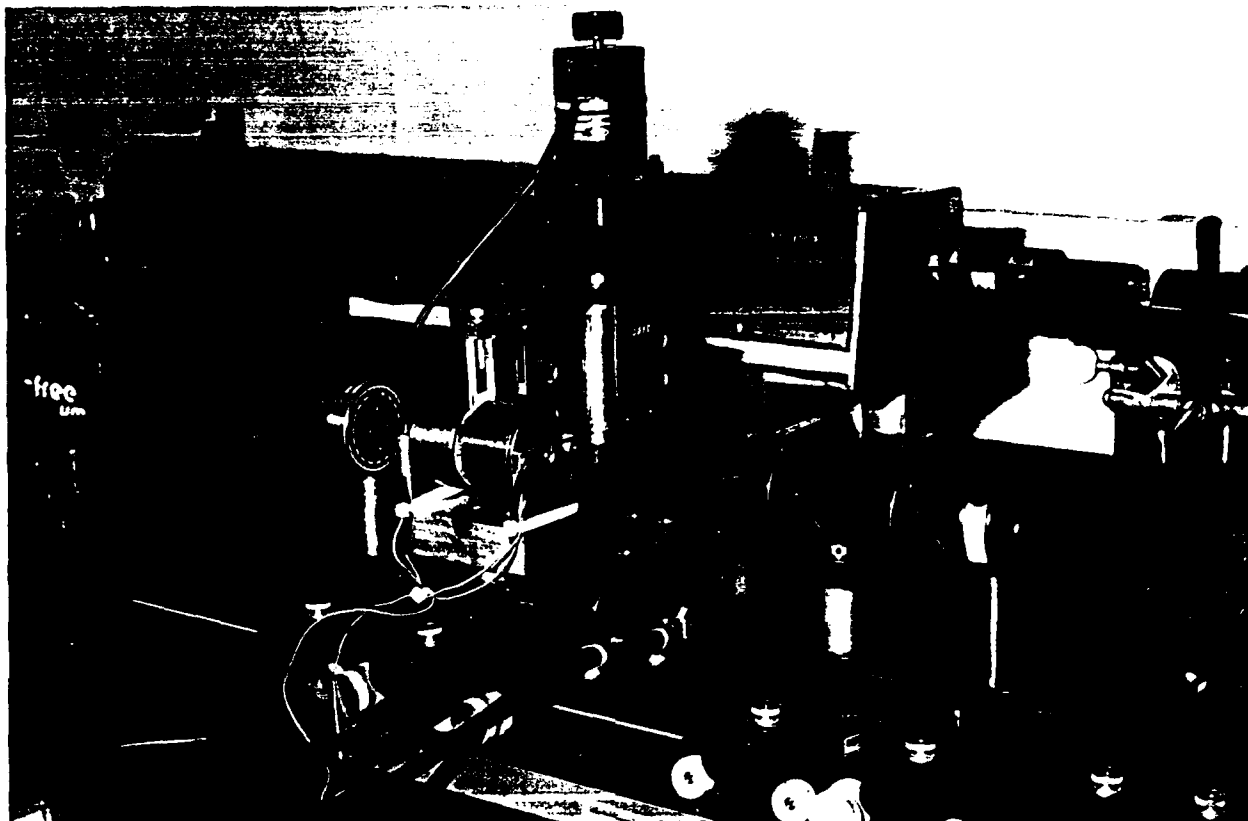


Figure 4. Split Magnet for FR Measurements.

The change in intensity of the probe beam caused by rotation of the plane of polarization (Faraday rotation) and propagation through the zinc selenide Brewster window analyzer was measured by a mercury cadmium telluride detector cooled to 77 K. All system components were located away from any stray magnetic fields that might have affected their performance. A high sensitivity lock-in amplifier, tuned to the modulating frequency of the magnetic field amplified the detector output and fed it into an IBM PC. The computer was programmed to automatically execute the sequences to control the scanning hardware and collect and reduce the data. Details of the software and theory of operation can be found in another report [3].

III. BACKGROUND THEORY

According to classical theory, at wavelengths long compared the bandgap wavelength, FR due to free carriers is given by [4]:

$$\delta = \lambda^2 B e^3 \frac{NL}{2\pi c^4 n m^{*2}} \quad (1)$$

a result that is well established for binary semiconductors. In Eq. (1) δ is the Faraday rotation angle in radians, $e = 4.8 \times 10^{-10}$ esu, the free carrier effective mass m^* was assumed to be 0.015m for MCT at 300 K, $m = 9.1 \times 10^{-28}$ gm, $n = 3.55 \times 10^{18}$ cm⁻³ is the free carrier concentration, $B = 2400$ Gauss, L and λ are the thickness of the sample and wavelength in units of cm, respectively, and π has its usual meaning. Using the following expression for the bandgap energy E_g given by Hansen et. al [5]:

$$E_g = -0.302 + 1.93x - 0.81x^2 + 0.832x^3 + 0.535 T \frac{(1-2x)}{1000} \quad (2)$$

where x = percent concentration of Cd, the band gap at $T = 300$ K for long wavelength IR MCT with $x = 0.200$ – 0.220 yields a cut-off wavelength = E_g (eV)/1.239 < 8 micrometers. Therefore the output from a CO₂ laser operating at 10.6 micrometers could be used for the probe beam for FR measurements at ambient temperature. We calculated the intrinsic carrier concentration $n(i)$, from the following expression given by Hansen and Schmit [6]:

$$n(i) = [5.585 - 3.82x + 1.753 (10^{-3})T - 1.364 (10^{-3}) x T] \left[(10^{14}) E_g^{3/4} T^{3/2} \exp \left(\frac{E_g}{2kT} \right) \right] \quad (3)$$

IV. RESULTS

Relative wafer sizes are shown in Figure 5 and the MCT thicknesses are given in Table 1 (shown in Section V).



Figure 5. Relative Sizes of MCT Used in FR Demonstration.
(MCT4 is of Similar Size But Not Shown).

MCT4 was reported to be n-type bulk grown by the traveling heater method and it was investigated in the most detail. The remaining three were supplied as LPE samples. Faraday rotation was proportional to the magnetic field strength B as expected from Eq. (1). Figure 6 shows the FR signal level plotted against B at an arbitrary position on MCT4. B was determined from the ac voltage across a 1 Ohm precision resistor in series with the magnet coils and from a direct measurement with a Gauss meter.

Figure 7 shows a comparison of normalized FR as a function of wafer position measured on different days and demonstrates that system repeatability was quite good. Laser fluctuations, although a potential source of scatter in the data do not appear to be a problem.

The magnitude of the Faraday rotation angle was measured directly by plotting the detector output as a function of θ , the angle through which the analyzer was rotated from parallel orientation to polarizer II ($\theta = 90^\circ$ would be the fully crossed position), Figure 3. A constant polarization reference plane was maintained for the radiation incident on a sample by rotating the analyzer and keeping the polarizers fixed. Figure 8 shows the optical train when no sample was in the beam. The beam was chopped at 10 Hz to provide a reference signal for the lock-in amplifier. Figure 9 shows the resulting detector output as a function of analyzer angle.

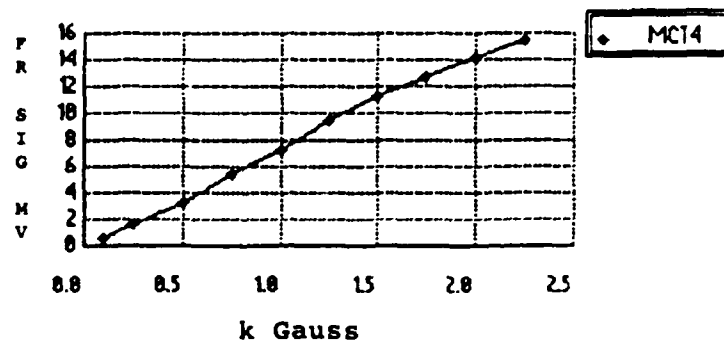


Figure 6. Faraday Rotation Signal vs Magnetic Field Strength.

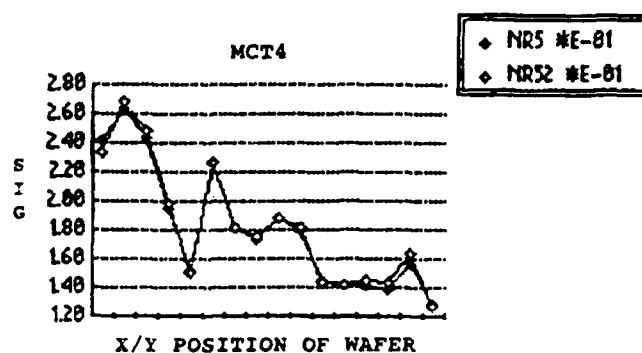


Figure 7. Faraday Rotation In MCT4 @ 300 K Repeatability Test.

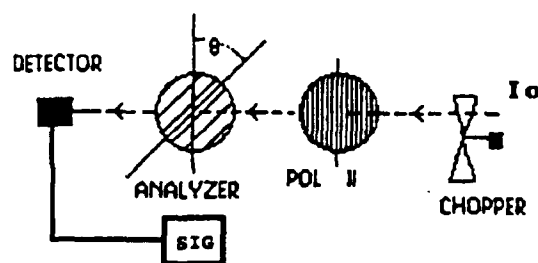


Figure 8. System Initialization Setup Without Sample.

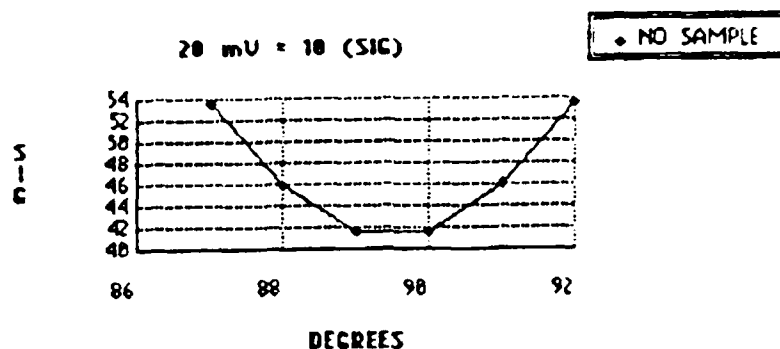


Figure 9. Detector Output vs Analyzer Angle - No Sample.

The chopper was turned off when a sample was in the modulated field and the amplitude modulated signal generated by Faraday rotation in the sample provided the ac signal necessary for the lock-in amplifier. With sample MCT4 in the modulated field the detector output had a maximum of near 87°, Figure 10. The difference between the maximum in Figure 9 corresponds to a FR of approximately 3 degrees.

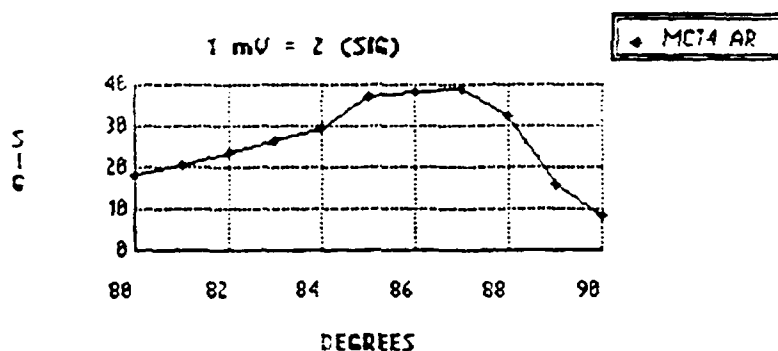


Figure 10. Faraday Rotation Signal vs Analyzer Angle for MCT4 at 300K.

A more analytical determination of the FR is obtained from the following analysis. From Beer's law and Malus' law the intensity I at the detector is given as

$$I = I_0 \exp(-aL) \cos^2(\theta + \delta) \quad (4)$$

where I_0 = intensity of the laser beam at polarizer II, a = absorption coefficient, L , δ , and θ are the wafer thickness, FR angle, and fixed angle between analyzer and polarizer, respectively.

The percent change in I can be found from Eq. (4) to be:

$$\frac{dI}{I} = 2\delta (d\delta) \tan (\theta + \delta) \quad (5)$$

Because there was no standard available to calibrate the FR system against, a representative value for the magnitude of the FR in MCT4 was calculated from Eq. (1) using the rotation angle determined as follows: A plot of the normalized Faraday rotation vs $\tan \theta$, (Reference Appendix), at an arbitrary position on the sample very closely approximates a straight line for θ less than about 80° , as expected from the small δ limit of Eq. (5). The departure from a straight line seen in Figure 11 for $\theta > 80^\circ$ is due to the contribution of δ .

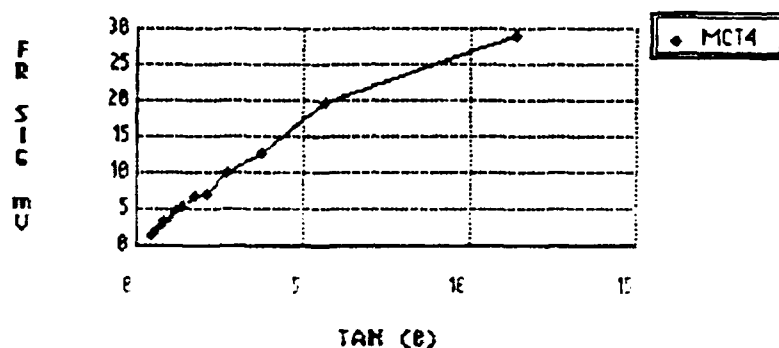


Figure 11. Faraday Rotation Signal vs Tangent of Analyzer Angle.

The small δ becomes a significant contributing factor as θ approaches 90 degrees because then the system sensitivity to FR theoretically approaches infinity, Eq. (5). In our measurements the gain in sensitivity from setting $\theta = 80^\circ$ instead of 45° was determined experimentally to be a factor of 4.5 compared to the theoretical value calculated from Eq. (5) i.e., $\tan (80/\tan (45) = 5.7$. The difference between the experimentally determined curve and the extrapolated $\tan (\theta)$ function yields a value of -3 degrees for δ , as Figure 12 shows, in good agreement with the value estimated directly from the relatively coarse scale marked in two degree increments on the analyzer holder.

Solving Eq. (1) for N yields $N = 6.7 (10^{15}) \text{ cm}^{-3}$ using [7] $n = 3.55$. The intrinsic free carrier concentration calculated from Eq. (3) is $n(i) = 2 * 10^{16}$ for $x = 0.22$ and $T = 300\text{K}$. No attempt was made to measure δ at a position in the wafer corresponding to the calculated mean value of N, only to show that δ obtained as described above is a reasonable value.

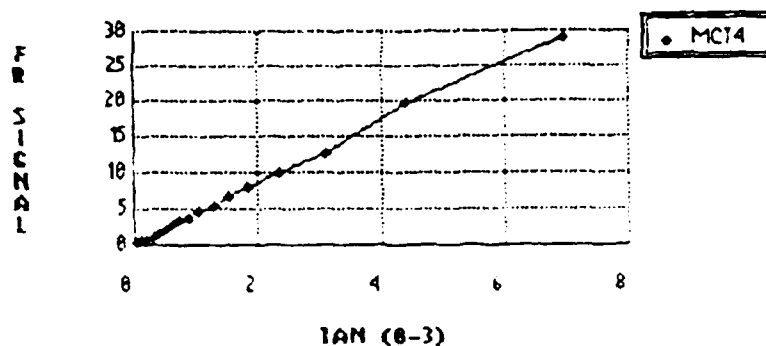


Figure 12. FR Signal vs Tan ($\theta - 3$).

The relative free carrier densities were measured in the bulk grown sample MCT4 at room temperature using the automated equipment developed in this laboratory. Figure 13 is a low resolution map of this sample generated from 20 data points and Figure 14 is a high resolution map of the same wafer generated from 63 data points. The acquisition time in both cases was approximately 20 sec/point. The analyzer angle θ was 80° . The free carrier concentration was found to vary 50% or more in sample MCT4. Although it may be desirable to perform measurements on cooled samples Nemiorovsky and Finkman [8] have pointed out that measurement of the intrinsic carrier concentration at room temperature can be used to determine the composition and band gap of n-type wafers if the wafer is known to be intrinsic at room temperature.

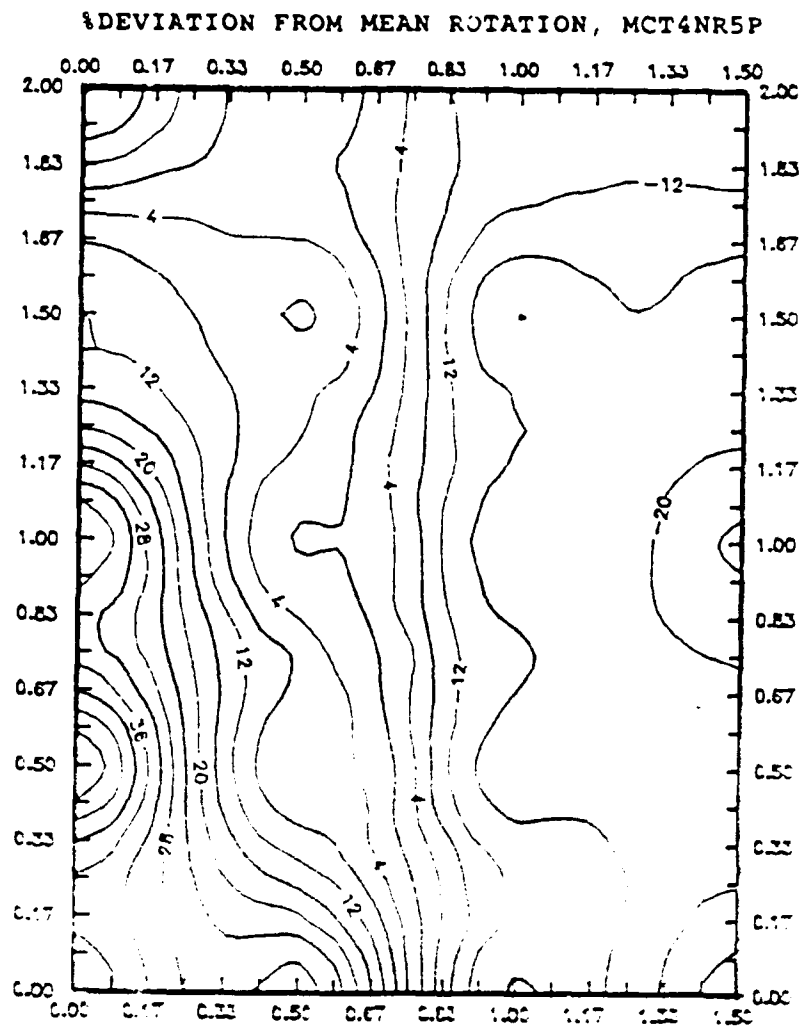


Figure 13. Low Resolution Map of MCT4 (20 Data Points).

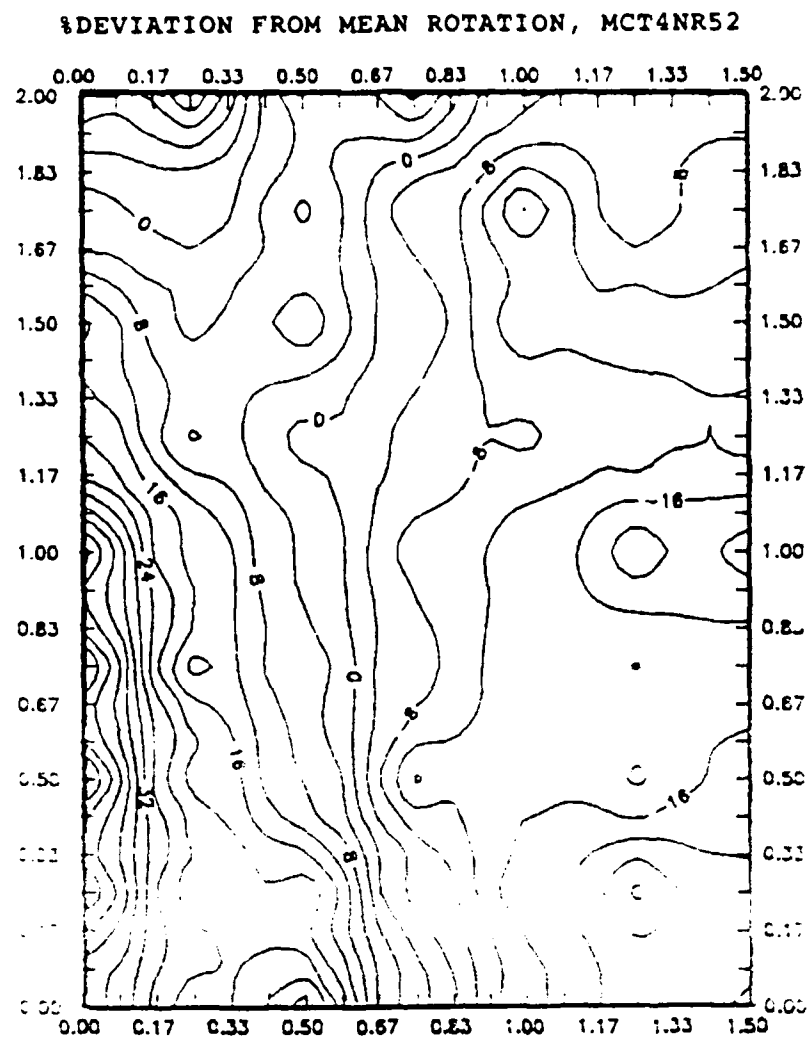


Figure 14. High Resolution Map of MCT4 (63 Data Points).

V. COMPARISONS

The relative amplitudes of the FR signal in n and p type LPE samples at 300K are compared in Table I with n-type bulk grown material. Table 1 also shows the free carrier concentrations at 77K determined by Hall measurements, although a direct comparison of FR with Hall results must be made at the same wafer temperature because of possible extrinsic effects.

TABLE 1. Relative Faraday Rotation Per cm in MCT @ 300K.

MCT#	TYPE	THICKNESS	N@ 77 K	FR(mV/cm)*	X
1	p-LPE	18 microns	1 E 17/cm ³	55.5	0.200-0.220
2	n-LPE	18 microns	2 E 14/cm ³	30.0	0.200-0.220
3	p-LPE	23 microns	8 E 15/cm ³	40.0	0.295
4	n-BULK	864 microns*	2 E 14/cm ³	31.8	0.200-0.220
Except where marked with *, samples and data in Table 1 were provided by Michael Grenn, CNVE0, U.S. Army CECOM.					

The significant features in Table 1 are:

1. The Faraday rotation per unit length (FR/cm) increased with increasing N as expected.
2. For a given N the magnitude of FR/cm was very close to the same value for n-type LPE and n-type bulk MCT. The FR results were virtually the same for both LPE and bulk grown material even though sample thicknesses differed by a factor of 48. This indicates that the method of growth made no significant difference in the Faraday rotation.

Possible extrinsic effects and other factors limit the extent to which one can compare Hall measurements made at 77K to these FR results made at 300K. However they appear to be in reasonable agreement and a direct comparison will be possible in the near future after FR measurements at 77K are completed.

VI. CONCLUSIONS AND RECOMMENDATIONS

Major conclusions and recommendations resulting from this effort are summarized as follows:

1. The feasibility of using the Faraday rotation technique to map free carrier concentrations in both bulk grown and epitaxially grown mercury cadmium telluride substrates was demonstrated here.
2. Qualitative results of FR are consistent with those reported for LPE and bulk grown n-type material.
3. In the limited circumstances of this first MCT FR mapping demonstration, the FR method appears to be a viable technique applicable to MCT. FR measurements at cryogenic temperatures on more samples are needed to demonstrate the full capability of this technique. FR agrees qualitatively with Hall measurements made independently, although comparisons of the average value of a high resolution map made at 300K with Hall measurements made at 77K are obviously very limited.
4. A calibration standard is needed to simplify absolute magnitude determinations.

REFERENCES

1. Balkansi, M. and Amzallag, E., Phys. Stat. Sol. 30,407, 1968.
2. Tanton, G. A., Grisham, J. A., Christensen, C. R. and Razi, S., "Proc. Electronics and E-O Materials for Smart Munitions Workshop." GACIAC, PR-87-01, pp. 105-114, Redstone Arsenal, AL, May 1987.
3. Stensby, J., A Computer Controlled System for Measurement of Faraday Rotation in Semiconductors, Technical Report for Contract No. DAAL03-86-D-0001, Delivery Order 1521, Scientific Services Program, USAMICOM, 1989.
4. Stephan, M. J. and Lidard, A.B., Journal of Physics and Chemistry of Solids, Vol. 9, p. 43, 1958.
5. Hansen, G. L. and Schmit, J. L., Journal of Applied Physics (USA), Vol. 54, No. 3, pp. 1639-1640, March 1983.
6. Brice, J. and Capper, P., Properties of Mercury Cadmium Telluride, INSPEC, The Institute of Electrical Engineers, The Gresham Press, 1987.
7. Nemirovsky, Y. and Finkman, E., Journal of Applied Physics (USA), Vol. 50, No. 12, pp. 8107-8111, December 1979.

APPENDIX
OPERATIONAL DETAILS OF THE FARADAY ROTATION
POLARIZER/ANALYZER COMBINATION

APPENDIX

OPERATIONAL DETAILS OF THE FARADAY ROTATION

POLARIZER/ANALYZER COMBINATION

The polarizer/analyzer combination forces the power incident on the detector to be proportional to $\cos^2\phi$, where ϕ is the angle between the analyzer's axis and the polarization axis of the radiation incident on the analyzer. Since the detectors' response was found to be linear within the operating range, this results in a detector output voltage which is also proportional to $\cos^2\phi$.

The polarizer/analyzer combination maps the FR-induced polarization modulation into an amplitude modulation that the detector/lock-in combination can respond to. The mapping is approximately linear if the polarizer/analyzer is operated near extinction, and the polarization modulation has a small peak value. This can be shown by setting

$$\phi = \frac{\pi}{2} + \theta_b + \delta \quad (\text{A-1})$$

where θ_b is a small constant bias term and δ is the FR which is periodic with fundamental frequency of 9 Hz. If $|\theta_b + \delta|$ is small, then the detector's output is proportional to

$$\cos^2 \left[\frac{\pi}{2} + \theta_b + \delta \right] = \sin^2 [\theta_b + \delta] = (\theta_b + \delta)^2 = \theta_b^2 + 2\theta_b\delta + \delta^2 \quad (\text{A-2})$$

The term $2\theta_b\delta$ is periodic with a frequency of 9 Hz, while $\theta_b^2 + \delta^2$ has only a DC and 18 Hz component.

The lock-in voltmeter, which is supplied a 9 Hz reference, responds to the component proportional to $2\theta_b\delta$. Hence, the voltmeter's response is referred to as the Absolute Rotation Signal (ARS) in what follows. The term proportional to $\theta_b^2 + \delta^2$ is filtered out by the meter. Note that the power incident on the detector is a function of sample transmission. This means that an ARS measurement is also dependent on sample transmission. However, transmission through the sample will be a function of position on the sample. Hence, an ARS measurement made at some position must be normalized by the transmission at the position so that the result, called the normalized Rotation Signal (NRS) in what follows, can be used to obtain the amount of rotation δ . How rotation δ is obtained from the NRS is discussed next.

The ARS is proportional to $2\theta_b\delta$; that is,

$$\text{ARS} = K \left[\cos^2 \left(\frac{\pi}{2} + \theta_b + \delta \right) \right] - K [\theta_b^2 + \delta^2] \quad (\text{A-3})$$

where K is a system constant depending on sample transmission, detector/amplifier gain, etc. The output of the detector when a transmission measurement is made (magnet off, chopper on) can be written as

$$K \left[\cos^2 \left(\frac{\pi}{2} + \theta_b \right) \right] m(t) = K [\theta_b^2] m(t), \quad (\text{A-4})$$

$$\text{where } m(t) = \begin{cases} 1 & 0 \leq t < \tau_0 \\ 0 & \tau_0 \leq t < T \end{cases}$$

and $m(t) = M(t+T)$, $-\infty < t < \infty$, is the T -periodic chopper function. The lock-in responds to the fundamental component of the detector's output. Now,

$$C_1 = \left(\frac{1.41}{\pi} \right) \left[1 - \cos \left(2\pi \frac{\tau_0}{T} \right) \right]^{\frac{1}{2}} \quad (\text{A-5})$$

is the magnitude of m 's fundamental component. Hence, during transmission measurements the lock-in reads

$$K c_1 \theta_b^2 = K \left\{ \left(\frac{1.41}{\pi} \right) \left[1 - \cos \left(\frac{2\pi \tau_0}{T} \right) \right]^{\frac{1}{2}} \right\} \theta_b^2 \quad (\text{A-6})$$

volts. This can be used to produce the normalized signal

$$NRS = \frac{K 2 \theta_b \delta}{K c_1 \theta_b^2} = \frac{2 \delta}{c_1 \theta_b} \quad (\text{A-7})$$

Finally, the rotation δ can be written as

$$\delta = 0.5 \theta_b c_1 NRS = 0.5 \theta_b \left\{ \left(\frac{1.41}{\pi} \right) \left[1 - \cos \left(\frac{2\pi \tau_0}{T} \right) \right]^{\frac{1}{2}} \right\} NRS \quad (\text{A-8})$$

an important result which was applied on empirical NRS measurements.

DISTRIBUTION LIST

AMSMI- RD	1 copy
AMSMI-RD-CS-R	15 copies
AMSMI-CS-T	1 copy
AMSMI-GC-IP, Mr. Fred M. Bush	1 copy
U.S. Army Materiel System Analysis Activity	1 copy
ATTN: AMXSY-MP (Herbert Cohen)	
Aberdeen Proving Ground, MD 21005	
IIT Research Institute	1 copy
ATTNN: GACIAC	
10 W. 35th Street	
Chicago, IL 60616	
AMSMI-RD-RE-OP, DR. Charles R. Christensen	100 copies
CECOM	2 copies
Center for Night Vision and Electro-Optics	
AMSEL-RD-NV-IT	
ATTN: Michael Grenn	
Bldg. 307	
Ft. Belvoir, VA 22060-5677	
Dr. Athanasios J. Syllaos	2 copies
Advanced Microelectronics Division	
Defense Systems & Electronics Group	
Texas Instruments	
P.O. Box 655474, MS 270	
Dallas, Texas 75265	
Bal K. Jindal	1 copy
Xacton	
P.O. Box 3129	
Tempe, Arizona 85281	

William C. Harsch
Miami Research Laboratories
Speciality Materials Division
Eagle-Pitcher Industries, Inc.
200 9th Ave. N E
Miami, Oklahoma 74354

2 copies

Dr. Lewis J. Hurt
U.S. Army Strategic Defense Command
ATTN: CSSD-H-LK
P. O. Box 1500
Huntsville, Alabama, 35807

1 copy